

Preface to Version 1

This report contains a description of computer programs prepared for the SCEC Stress-Triggering and Deformation Software Training Workshop held September 7-9, 1999 at Stanford University. The program package, VISCO1D, is designed to handle computation of deformation fields related to postseismic relaxation in situations commonly encountered in practice. For example, they are well suited for calculating postseismic deformation at Earth's surface following large crustal earthquakes for comparison with local or regional geodetic data. This report is separated into two parts: MANUAL and TUTORIAL. In the MANUAL it is my intention to give the necessary theoretical background for understanding what problem the programs are actually solving. In the TUTORIAL, I attempt to give prospective users sufficient familiarity with the programs that they will be able to run them independently. The example problems were chosen to bring out the variety of problems that can be solved with VISCO1D.

Acknowledgments. The computer programs described here were written mostly during my time at the Carnegie Institute of Washington, Department of Terrestrial Magnetism as a postdoctoral fellow from 1989 to 1992. Further work was done while I was a postdoctoral fellow at the University of Cambridge, Institute of Theoretical Geophysics from 1995 to 1997. I thank the many colleagues at those institutions for their encouragement and stimulation. Special thanks are due to Selwyn Sacks of CIW/DTM for generating my initial interest in postseismic relaxation problems and for convincing me that their potential for research applications would inexorably grow in step with the observational database.

I thank Nancy Sandoval and Ross Stein of the U.S.G.S., and hosts Phil Farrell and Paul Segall of Stanford University for their organizational efforts in making this software workshop a reality.

I thank the students at UC Davis for helping me prepare the tutorial, and Louise Kellogg, Doug Neuhauser, and Paul Waterstraat of UC Davis for helping me set up the material on the internet.

Fred Pollitz

August 20, 1999

Preface to Version 2

In the 3 1/2 years since the original distribution of the programs, a few improvements have been made. These are:

(1) In the conversion from slip values to moment tensor components, the old version assumed a constant (internally specified) shear modulus. The current version uses the correct depth-dependent values of elastic moduli (i.e., those specified in 'earth.model') to make this conversion.

(2) The old VTORDEP and VSPHDEP compute exact values of mode eigenfunctions at 10 depth points within the upper elastic layer and store them in their respective output files. Cubic spline interpolation is then used by STRAINX and STRAINW to obtain the function values elsewhere. Subsequent testing has shown that small errors are introduced by the interpolation process. The new version uses 40 depth points to represent the mode eigenfunctions.

The combined effect of the above two changes means that values of displacement and strain computed by the new version will differ from those of the old version by a few %. Bear this in mind when running the example problems in the tutorial and comparing with the printed 'old' results.

(3) In the source codes, old fortran commands such as "dfloat" and "float" have been replaced by newer commands which are better compatible with most platforms.

(4) An automatic criterion for ensuring stable mode computation has been revised. The old criterion was "too reliable", removing too many well-determined modes from the basis set.

(5) Several typos in the equations have been corrected.

(6) A new section has been added to address validation of VISCO1D.

Fred Pollitz
May 8, 2003

MANUAL

VISCO1D is a program package designed to describe the response of a spherically stratified elastic-viscoelastic medium to the stresses generated by an earthquake occurring in one of the elastic layers. The response is described in a spherical earth geometry in terms of a spherical harmonic expansion of spheroidal and toroidal motion components, each component representing one "mode" of relaxation with its own characteristic decay time and spatial deformation pattern. It is highly flexible and allows the determination of time-dependent postseismic deformation fields (three components of displacement and six independent components of strain) at any depth level. It handles shear dislocations on a specified fault plane, or extension across a specified fault plane. Use of the program package consists of four main parts:

1. Specification of a stratified Earth model (elastic moduli and viscosity of every layer).
2. Identification of spheroidal and toroidal motion modes on this Earth model, consisting of a set of characteristic decay times for each spherical harmonic degree.
3. Determination of the corresponding displacement-stress vectors for each of these modes.
4. Determination of postseismic deformation at specified times, observation points (lat,lon,depth), and source geometry and slip.

There are two sets of programs, one designed for non-gravitational viscoelastic response and the other for gravitational viscoelastic response. The former runs considerably faster.

(1) Theoretical Background

Pollitz [1992] gave an analytic formulation for the time-dependent postseismic relaxation on a spherically layered viscoelastic Earth model, in the absence of gravitational relaxation, and Pollitz [1997] extended this to the case of gravitational viscoelastic relaxation. The following summarizes the methods given in those papers.

We work in a spherical (r, ϑ, φ) epicentral coordinate system such that $\vartheta = 0$ corresponds to the source epicenter S (Figure 1). Variables ϑ and φ then denote the angular distance and azimuth (taken positive counterclockwise from due South) from the source epicenter to the observation point. For a layered elastic-viscoelastic rheology, the correspondence principle can be applied to the equations of static equilibrium to yield a solution which may be expanded in terms of normal modes. These solutions

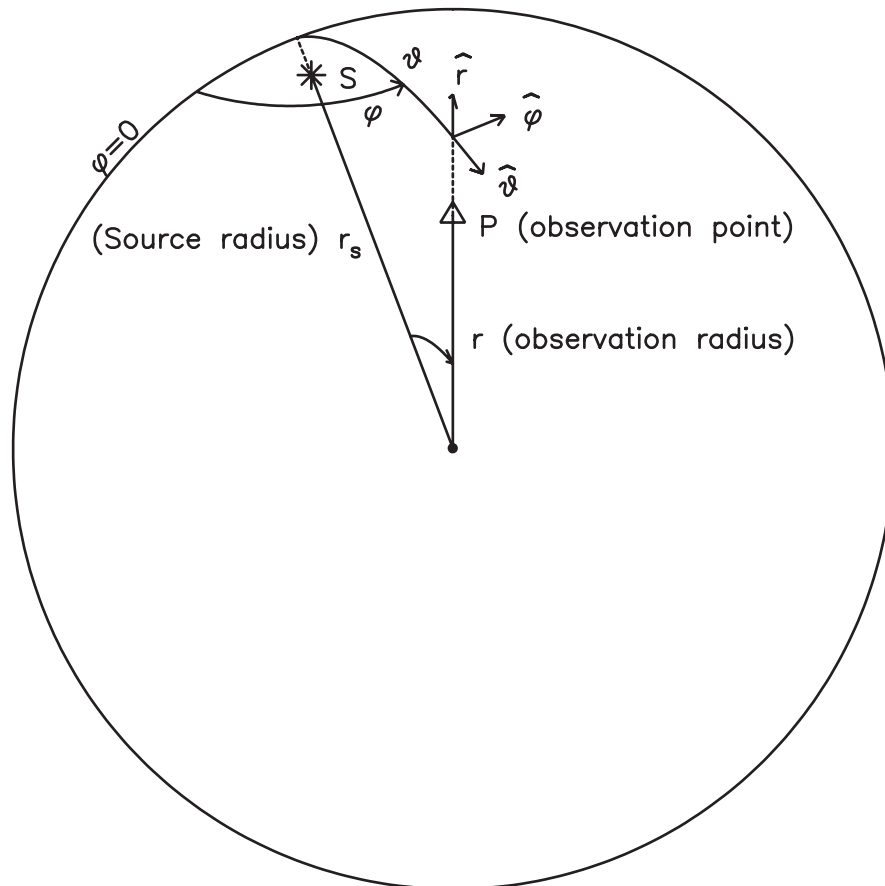


Figure 1.
Spherical
Geometry

are separable into spheroidal and toroidal modes.

The correspondence principle allows us to express the Laplace-transformed solutions of the equations of static equilibrium into solutions of the untransformed equations of equilibrium provided that shear modulus μ and bulk modulus κ take the form

$$\begin{aligned}\mu(r, s) &= \frac{\mu(r) s}{s + \mu(r)/\eta(r)} \\ \kappa(r, s) &= \kappa(r)\end{aligned}\tag{1}$$

where $\mu(r)$, $\kappa(r)$, and $\eta(r)$ are the spherically symmetric distribution of shear modulus, bulk modulus, and viscosity, respectively. Equation (1) is appropriate for a **Maxwell viscoelastic fluid** rheology. The second of equations (1) means that only relaxation in shear is considered here. Equation (1) implies that at long times after a stress perturbation, corresponding to the limit $s \rightarrow 0$, effective shear strength will approach zero, i.e. the material will possess no shear strength. Cohen [1982, Appendix] has given the stress–strain relations for the time–dependent deformation of a **standard linear solid**, consisting of a purely elastic element with rigidity μ_a in series with a Kelvin element, which consists of an elastic element with rigidity μ_b in parallel with a viscous element of viscosity η . This rheology allows for a long-term shear strength μ' equal to

$$\mu' = \frac{\mu_a \mu_b}{\mu_a + \mu_b}\tag{2}$$

The correspondence principle for a standard linear solid takes the form (equation (4) of Pollitz and Sacks, 1996)

$$\begin{aligned}\mu(s) &= \frac{\mu_a s + \mu' \tau^{-1}}{s + \tau^{-1}} \\ \kappa(r, s) &= \kappa(r)\end{aligned}\tag{3}$$

where $\tau = \eta / (\mu_a + \mu_b)$. Clearly this reduces to a Maxwell viscoelastic fluid when $\mu_b = 0$.

Let $\rho_0(r)$, $\mu(r)$, and $\kappa(r)$ denote the density, shear modulus, and bulk modulus, respectively, on a spherically symmetric reference Earth model, and let $\phi_0(r)$ denote

the corresponding gravitational potential. After an earthquake the Earth moves from its initial state of equilibrium, and we define the perturbed density and gravitational potential at $\mathbf{r} = (r, \theta, \phi)$ and time t as

$$\begin{aligned}\rho(\mathbf{r}, t) &= \rho_0(r) + \rho_1(\mathbf{r}, t) \\ \phi(\mathbf{r}, t) &= \phi_0(r) + \phi_1(\mathbf{r}, t)\end{aligned}\quad (4)$$

Let a source with moment tensor $\mathbf{M}(t)$ be located at \mathbf{r}_s . Denoting the displacement field with $\mathbf{u}(\mathbf{r}, t)$ and the corresponding elastic stress tensor with $\mathbf{T}(\mathbf{r}, t)$, the linearized equations of static equilibrium are

$$\begin{aligned}-\rho_0 \nabla \phi_1 - \rho_1 \nabla \phi_0 - \nabla[\rho_0 \mathbf{u} \cdot \nabla \phi_0] + \nabla \cdot \mathbf{T} &= \mathbf{M}(t) : \nabla \delta(\mathbf{r} - \mathbf{r}_s) \\ \rho_1 &= -\nabla \cdot (\rho_0 \mathbf{u}) \\ \nabla^2 \phi_1 &= 4\pi G \rho_1 \\ \mathbf{T} &= (\kappa - \frac{2}{3}\mu) (\nabla \cdot \mathbf{u}) \mathbf{I} + 2\mu \boldsymbol{\varepsilon} \\ \nabla^2 \phi_0 &= 4\pi G \rho_0\end{aligned}\quad (5)$$

Equations (5) are equivalent to equations (1), (2), (10), and (11) of Dahlen [1972] without the inertial and rotational terms. The fourth equation in (5) assumes an isotropic elastic medium. Except at the source radius, where the following quantities may be discontinuous, equations (5) are to be solved subject to the boundary conditions (1) \mathbf{u} is continuous except at fluid-solid boundaries where $\hat{\mathbf{r}} \cdot \mathbf{u}$ must be continuous, (2) $\hat{\mathbf{r}} \cdot \mathbf{T}$ is continuous, (3) ϕ_1 is continuous, and (4) $\hat{\mathbf{r}} \cdot \nabla \phi_1 + 4\pi G \rho_0 \hat{\mathbf{r}} \cdot \mathbf{u}$ is continuous. In (5), $\boldsymbol{\varepsilon}$ is the strain tensor

$$\boldsymbol{\varepsilon} = \frac{1}{2} \left[(\nabla \mathbf{u}) + (\nabla \mathbf{u})^T \right] \quad (6)$$

\mathbf{I} is the 3x3 identity matrix, and G is the gravitational constant. Defining the gravitational acceleration on the reference Earth model as

$$\mathbf{g}_0 = -g_0 \hat{\mathbf{r}} = -\nabla \phi_0 \quad (7)$$

we may rewrite the first of (5) as

$$-\rho_0 \nabla \phi_1 - \rho_1 \nabla \phi_0 - \nabla[(\hat{\mathbf{r}} \cdot \mathbf{u}) \rho_0 g_0] + \nabla \cdot \mathbf{T} = \mathbf{M}(t) : \nabla \delta(\mathbf{r} - \mathbf{r}_s) \quad (8)$$

Viscoelasticity may be introduced at this stage. Defining the Laplace transform of a function $f(t)$ via

$$\tilde{f}(s) = \int_0^{\infty} f(t) e^{-st} dt$$

the equations of quasi-static equilibrium may be obtained via the correspondence principle, taking the Laplace transform of (5) and replacing $\mu(r)$ and $\kappa(r)$ with the expressions in (1) or (3). In particular, the first of (5) takes the form

$$-\rho_0 \nabla \tilde{\phi}_1 - \tilde{\rho}_1 \nabla \phi_0 - \nabla [(\hat{\mathbf{r}} \cdot \tilde{\mathbf{u}}) \rho_0 g_0] + \nabla \cdot \tilde{\mathbf{T}} = \frac{1}{s} \mathbf{M} : \nabla \delta(\mathbf{r} - \mathbf{r}_s) \quad (9)$$

In (9) it has been assumed that the source acts as a step function in time and that it is embedded in a purely elastic medium.

The first three terms on the left-hand side of (9) depend explicitly on either g_0 or G . The third term contains a dependence on both after noting that

$$\nabla g_0 = \left[-\frac{2}{r} g_0 + 4\pi G \rho_0 \right] \hat{\mathbf{r}} \quad (10)$$

The first term on the left-hand side of (9) scales as $4\pi G \rho_0^2 |\mathbf{u}|$, and from (10) the G dependent part of the third term scales similarly. Strain scales as $|\mathbf{u}|/\text{wavelength}$ and the gradient of strain scales as $|\mathbf{u}|/(\text{wavelength})^2$. The relative importance of G terms and elastic terms in the force balance (9) is then given by the dimensionless ratio

$$\frac{4\pi G \rho_0^2 |\mathbf{u}|}{(\kappa \text{ or } \mu)(|\mathbf{u}|/(\text{wavelength})^2)} = \frac{4\pi G \rho_0^2 (\text{wavelength})^2}{\kappa \text{ or } \mu}$$

Using typical parameter values in the upper mantle, this ratio equals 0.05 at wavelength 400 km and diminishes rapidly at shorter wavelength. A similar scaling analysis for the relative importance of G terms and g terms in equation (9) shows that this is governed by the ratio

$$\frac{4\pi G \rho_0^2 |\mathbf{u}|}{\rho_0 g_0 (|\mathbf{u}|/(\text{wavelength}))} = \frac{4\pi G \rho_0 (\text{wavelength})}{g_0}$$

This ratio equals about 0.10 at 400 km wavelength. Since most observational constraints on postseismic relaxation correspond to wavelengths shorter than 400 km, the neglect of G terms in (9) is an excellent approximation. This scaling analysis remains

valid even in the relaxed limit because the elastic term proportional to $\kappa(\nabla \cdot \mathbf{u})$ is non-negligible. Justification of the neglect of perturbations in gravitational potential for postseismic relaxation calculations on a layered half-space was previously discussed by Rundle [1981]. The equations of quasi-static equilibrium then reduce to

$$\begin{aligned} \rho_0 g_0 \left[((\nabla \cdot \tilde{\mathbf{u}}) + \frac{2}{r} (\hat{\mathbf{r}} \cdot \tilde{\mathbf{u}})) \hat{\mathbf{r}} - \nabla(\hat{\mathbf{r}} \cdot \tilde{\mathbf{u}}) \right] + \nabla \cdot \tilde{\mathbf{T}} &= \frac{1}{s} \mathbf{M} : \nabla \delta(\mathbf{r} - \mathbf{r}_s) \\ \tilde{\rho}_1 &= -\nabla \cdot (\rho_0 \tilde{\mathbf{u}}) \\ \tilde{\mathbf{T}} &= \kappa(r, s) (\nabla \cdot \tilde{\mathbf{u}}) \mathbf{I} + 2\mu(r, s) \tilde{\boldsymbol{\varepsilon}} \\ \nabla^2 \phi_0 &= 4\pi G \rho_0 \end{aligned} \quad (11)$$

with the surface boundary condition

$$\hat{\mathbf{r}} \cdot \tilde{\mathbf{T}} = 0 \quad r = R \quad (12)$$

and an appropriate lower boundary condition in the Earth's interior. In the following the notation \tilde{f} will be dropped and the argument t or s will indicate evaluation in the time domain or Laplace transform domain, respectively.

In the normal mode method, (11) are solved as a superposition of normal modes, each of which satisfies (11) without the source term (proportional to \mathbf{M}), with excitation coefficients which depend on the moment tensor and source depth. I will provide details of this solution for the case of spheroidal modes, and then quote the appropriate results for the toroidal modes.

1.1 Spheroidal Motion Solution

The total spheroidal mode displacement field which solves (11) can be expanded as a sum of normal modes in the form [Pollitz, 1992, equation (18)]

$$\begin{aligned} \mathbf{u}_S(\mathbf{r}, s) &= \sum_n \sum_{l=0}^{\infty} \sum_{m=0}^2 \frac{\left[{}_n y_{1l}(r, s) \hat{\mathbf{r}} + {}_n y_{3l}(r, s) \nabla_1 \right]}{{}_n (I_1)_l ({}_n \omega_l)^2} \\ &\quad \Sigma_{m+1}(\phi, s) (-1)^m X_l^m(\theta) (1/s) \end{aligned} \quad (13)$$

The corresponding traction on spherical shells of radius r can be written

$$\hat{\mathbf{r}} \cdot \mathbf{T}_S(\mathbf{r}, s) = \sum_n \sum_{l=0}^{\infty} \sum_{m=0}^2 \frac{\left[{}_n y_{2l}(r, s) \hat{\mathbf{r}} + {}_n y_{4l}(r, s) \nabla_1 \right]}{{}_n (I_1)_l ({}_n \omega_l)^2} \quad (14)$$

$$\Sigma_{m+1}(\phi, s) (-1)^m X_l^m(\theta) (1/s)$$

In (13) and (14), ∇_1 is the surface gradient operator

$$\nabla_1 = \frac{\partial}{\partial \theta} \hat{\theta} + \frac{1}{\sin \theta} \frac{\partial}{\partial \phi} \hat{\phi}$$

and the y_{jl} are components of a displacement-stress vector

$${}_n \mathbf{y}_l = \begin{bmatrix} {}_n y_{1l} \\ {}_n y_{2l} \\ {}_n y_{3l} \\ {}_n y_{4l} \end{bmatrix} \quad (15)$$

The Σ functions are mode excitation functions which contain the dependence on the source depth r_s , the moment tensor, and the source-observation point azimuth ϕ . They are given by [Pollitz, 1992]

$$\begin{aligned} \Sigma_1 &= \left[\frac{l+1/2}{2\pi} \right]^{1/2} \left[M_{rr} \partial_r y_1 + (M_{\phi\phi} + M_{\theta\theta}) r_s^{-1} \left[y_1(r_s) - \frac{1}{2} [l(l+1)] y_3(r_s) \right] \right] \\ \Sigma_2(\phi) &= \left[\frac{l+1/2}{2\pi} \right] [l(l+1)]^{1/2} (M_{r\theta} \cos\phi + M_{r\phi} \sin\phi) [\partial_r y_3(r_s) + r_s^{-1} (y_1(r_s) - y_3(r_s))] \\ \Sigma_3(\phi) &= \left[\frac{l+1/2}{2\pi} \right] [l(l+1)(l-1)(l+2)]^{1/2} \\ &\quad \times \left[\frac{1}{2} (M_{\theta\theta} - M_{\phi\phi}) \cos 2\phi + M_{\theta\phi} \sin 2\phi \right] r_s^{-1} y_3(r_s) \end{aligned} \quad (16)$$

$X_l^m(\theta)$ is a Legendre function defined by $Y_l^m(\theta, \phi) = X_l^m(\theta) \exp [im\phi]$, where $Y_l^m(\theta, \phi)$ is a fully normalized spherical harmonic of degree l . Variable ${}_n (I_1)_l$ is the kinetic energy integral given by equation (11) of Pollitz [1992] and ${}_n \omega_l$ is the corresponding frequency for the n th dispersion branch with spherical harmonic degree l ; these two factors also depend on s .

In layer v at a fixed l , \mathbf{y}_l satisfies an equation of the form [Takeuchi and Saito, 1972]

$$\frac{d\mathbf{y}_l(r)}{dr} = \mathbf{A}_{lv}(r) \mathbf{y}_l(r) \quad (17)$$

Two independent solutions $\mathbf{y}_l^{(I)}$ and $\mathbf{y}_l^{(II)}$ are integrated upward layer by layer from an appropriate starting radius to the surface $r = R$. Stress-free boundary conditions require that there exists a linear combination of these two solutions with vanishing shear and normal stress. This yields the free surface boundary condition

$$(\mathbf{y}_l^{(1)}(R))_2 \times (\mathbf{y}_l^{(2)}(R))_4 - (\mathbf{y}_l^{(1)}(R))_4 \times (\mathbf{y}_l^{(2)}(R))_2 = 0 \quad (18)$$

The subscripts 2 and 4 in (18) refer to shear and normal stress components, respectively, of the displacement-stress vectors.

In the nongravitational case, \mathbf{y}_l is a 4×1 column vector and \mathbf{A}_{lv} is a 4×4 matrix which depend on the transformed elastic moduli of layer v and the spherical harmonic degree l . Since the functions I_1 are positive for all modes, the poles of $\mathbf{u}(r, s)$ occur at values $s = -s_j$ for which $\omega^2(s) = 0$. Consider, for example, the r component of the displacement field. Assuming that all of the poles are simple poles (which is proved below), then the Laplace transformed displacement field can be rewritten in the form

$$\hat{\mathbf{r}} \cdot \mathbf{u}_S(\mathbf{r}, s) = {}_r \mathbf{u}_S^0(\mathbf{r}) \frac{1}{s} + \sum_j \frac{{}_r \gamma_S)_j(\mathbf{r})}{s + s_j} \frac{1}{s} \quad (19)$$

In general, each displacement component of total degree l has an associated set of poles $\{s_j\}$ used in the evaluation of (19). At fixed l , the coefficient $({}_r \gamma_S)_j(\mathbf{r})$ in (18) equals the residue of the expression within the summation of (13) evaluated at $s = -s_j$.

$$({}_r \gamma_S)_j(\mathbf{r}) = y_1(r) \frac{\sum \left[\Sigma_{m+1}(\phi, s) X_l^m(\theta) (-1)^m \right]}{I_1(s) \frac{d}{ds} \omega^2(s) \Big|_{s=-s_j}} \quad (20)$$

An expression for $(d/ds)\omega^2(s)$ is given by Pollitz [1992, equations (22)-(25)]. Since publication of that paper I have used an alternative equivalent expression which uses μ and κ as independent variables and brings out the fact that $(d/ds)\omega^2(s)$ is always positive

$$\varepsilon_j = I_1(s) \frac{d}{ds} \omega^2(s) \Big|_{s=-s_j} = \int_0^R I_1 \left[\frac{\partial \omega^2}{\partial \mu} \right] \Big|_{\kappa} \frac{\partial \mu(r, s)}{\partial s} dr \quad (21)$$

where [Romanowicz, 1987, Appendix I]

$$I_1 \left[\frac{\partial \omega^2}{\partial \mu} \right] \Big|_{\kappa} = \left[\frac{1}{3} (2\partial_r y_1(r, s) - F)^2 + L(\partial_r y_3(r, s) + r^{-1}(y_1(r, s) - y_3(r, s)))^2 + (r^{-1}y_3(r, s))^2 (2(L - 1)L - L^2) \right] r^2$$

$$F = r^{-1} (2y_1(r, s) - l(l+1) y_3(r, s)) \quad (22)$$

$$L = l(l+1)$$

The corresponding term proportional to $[\partial \omega^2 / \partial \kappa] \Big|_{\mu}$ is omitted because $(\partial / \partial s) \kappa(r, s) = 0$ from equation (1); the derivative $(\partial / \partial s) \mu(r, s)$ which appears in the integrand in (21) is readily calculated from (1). Equation (22) combined with the fact that $I_1(s) > 0$ and $(\partial / \partial s) \mu(r, s) > 0$ for real-valued s proves that $(d/ds) \omega^2(s)$ is always positive, which proves that the poles of (13) are simple poles. It should be pointed out that in the gravitational case the integrand given in (21) has precisely the same form as in the nongravitational case (that is, no additional terms proportional to g_0 are introduced into (22)).

The inverse Laplace transform of (19) has the form

$$\hat{\mathbf{r}} \cdot \mathbf{u}_S(\mathbf{r}, t) = {}_r \mathbf{u}_S^0(\mathbf{r}) H(t) + \sum_j \frac{({}_r \gamma_S)_j(\mathbf{r})}{s_j} [1 - e^{-s_j t}] \quad (23)$$

where $H(t)$ is the Heaviside step function. The term proportional to $H(t)$ in (23) represents the coseismic displacement field and will be dropped from now on in order to concentrate on the postseismic displacement fields represented by the summation term in that equation. Going through the same procedure for all three displacement components yields an expression for the total postseismic displacement field of the form

$$\mathbf{u}_S(\mathbf{r}, t) = \sum_j [({}_r \gamma_S)_j(\mathbf{r}) \hat{\mathbf{r}} + ({}_\theta \gamma_S)_j(\mathbf{r}) \hat{\boldsymbol{\theta}} + ({}_\phi \gamma_S)_j(\mathbf{r}) \hat{\boldsymbol{\phi}}] \times \frac{1 - e^{-s_j t}}{s_j} \quad (24)$$

where the γ functions for a point source with a given moment tensor are given by [Pollitz, 1992, equation (27)].

$$\begin{aligned}
 ({}_r\gamma_S)_j(\mathbf{r}) &= y_1(r, -s_j) \sum_{m=0}^2 \left[\Sigma_{m+1}(\phi, s) X_l^m(\theta) (-1)^m \right] \boldsymbol{\varepsilon}_j^{-1} \\
 ({}_\theta\gamma_S)_j(\mathbf{r}) &= y_3(r, -s_j) \sum_{m=0}^2 \left[\Sigma_{m+1}(\phi, s) \partial_\theta X_l^m(\theta) (-1)^m \right] \boldsymbol{\varepsilon}_j^{-1} \\
 ({}_\phi\gamma_S)_j(\mathbf{r}) &= y_3(r, -s_j) \sum_{m=1}^2 \left[\partial_\phi \Sigma_{m+1}(\phi, s) X_l^m(\theta) (-1)^m \right] \boldsymbol{\varepsilon}_j^{-1} (\sin\theta)^{-1}
 \end{aligned} \tag{25}$$

We may now address the character of the solutions of (17). In the nongravitational case, assuming fixed l , the solution of (17) in layer v can be written in powers of r [Pollitz, 1992]

$$\begin{aligned}
 \mathbf{y}_v(r) &= c_1 \text{diag} (r^{l+1} \ r^l \ r^{l+1} \ r^l) \mathbf{p}_{1v} \\
 &+ c_2 \text{diag} (r^{l-1} \ r^{l-2} \ r^{l-1} \ r^{l-2}) \mathbf{p}_{2v} \\
 &+ c_3 \text{diag} (r^{-l} \ r^{-l-1} \ r^{-l} \ r^{-l-1}) \mathbf{p}_{3v} \\
 &+ c_4 \text{diag} (r^{-l-2} \ r^{-l-3} \ r^{-l-2} \ r^{-l-3}) \mathbf{p}_{4v}
 \end{aligned} \tag{26}$$

The $\{\mathbf{p}_{i v}\}$ in (26) are column vectors which depend only on the elastic moduli in layer v , the c_i are arbitrary constants, and *diag* denotes the 4×4 matrix consisting of the specified diagonal elements and zero off-diagonal elements. In the gravitational case, a 6×6 matrix specified by Takeuchi and Saito [1972] and given by Pollitz [1992, equation (43)] determines the layer deformation. However, our discussion of the G terms of (9) showed that coupling with the perturbations in gravitational potential is negligible, and then $\mathbf{A}_{l v}$ is given by the upper left 4×4 submatrix of this matrix:

$$\mathbf{A}_{l v}(r, s) = \begin{bmatrix} -2\lambda\sigma^{-1}r^{-1} & \sigma^{-1} & \lambda\sigma^{-1}l(l+1)r^{-1} & 0 \\ -4\rho gr^{-1}+4\gamma r^{-2} & 2(\lambda\sigma^{-1}-1)r^{-1} & (-2\gamma r^{-2}+\rho gr^{-1})l(l+1) & l(l+1)r^{-1} \\ -r^{-1} & 0 & r^{-1} & \mu^{-1} \\ \rho gr^{-1}-2\gamma r^{-2} & -\lambda\sigma^{-1}r^{-1} & -2\mu r^{-2}+(\gamma+\mu)l(l+1)r^{-2} & -3r^{-1} \end{bmatrix}$$

$$\begin{aligned}
 \mu &= \mu_v(s) \\
 \lambda &= \lambda_v(s) = \kappa_v(s) - \frac{2}{3} \mu_v(s) \\
 \sigma &= \lambda_v(s) + 2 \mu_v(s) \\
 \gamma &= \lambda_v(s) + \mu_v(s) - \lambda_v^2(s) \sigma^{-1}
 \end{aligned} \tag{27}$$

Rundle [1982] and Iwasaki [1985] incorporated gravitation effects into their respective half-space formulations by assuming constant gravitational acceleration g , which is an excellent approximation for that part of the Earth which influences near-field crustal deformation (namely, this approximation accounts well for the weight of the thin upper lithospheric plate and any restoring force at the lithosphere/asthenosphere boundary). Similarly, I will assume that the product $\rho_0 g_0$ varies with radius according to

$$\rho_0(r) g_0(r) = \frac{\text{constant}}{r} \quad (28)$$

Agreement with the actual $\rho_0(r)g_0(r)$ in the Earth can be enforced as accurately as necessary by dividing the crust and mantle into as many layers as necessary. This can be done with small error by employing single layers for the upper crust and lower crust. An appropriate choice of the constant in (28) is found to match the contrast in $\rho_0 g_0$ at the crust/mantle boundary and accommodate about one-half of the increase in the actual $\rho_0(r) g_0(r)$ on Model 1066A [Gilbert and Dziewonski, 1975] in the entire upper mantle; thus it is, to a first approximation, better than a model assigning constant density and gravitational acceleration to the upper mantle.

With this approximation, it is then straightforward to represent the deformation in a layer as a sum of four independent solutions which depend on powers of r . Under the above assumptions the solution to (17) may be written in the form

$$\begin{aligned} \mathbf{y}_v(r) &= \mathbf{P}_v(r, r_0) y_v(r_0) \\ \mathbf{P}_v(r, r_0) &= \text{diag} [r, 1, r, 1] \exp \left\{ (\tilde{\mathbf{A}}_v - \text{diag} [1, 0, 1, 0]) \ln \frac{r}{r_0} \right\} \\ &\quad \times \text{diag} [r_0^{-1}, 1, r_0^{-1}, 1] \end{aligned} \quad (29)$$

where $\tilde{\mathbf{A}}_v$ is equal to \mathbf{A}_v with all appearances of r removed, and r_0 is an arbitrary reference radius, The propagator matrix \mathbf{P}_v has the property $\mathbf{P}_v(r, r) = \mathbf{I}$, the identity matrix, and the elements of $y_v(r)$ depend upon powers of r like r^{p+1} (displacement components) and r^p (stress components), where p is one of the eigenvalues of $\tilde{\mathbf{A}}_v - \text{diag} [1, 0, 1, 0]$. In the nongravitational case, these eigenvalues are $p = l, l-2$,

$-l-1$, and $-l-3$, which leads to equivalence with the representation (26). The matrix exponential required in (29) can be calculated either directly using a scaled Taylor's expansion or with an eigenvalue expansion in powers of r .

In the implementation of this algorithm, an analytic solution for the deformation of a homogeneous sphere is applied at either the lowest depth specified in the earth model depths deep (one wavelength equals $2\pi R/(l+1/2)$, where R is Earth's radius and l is the total degree number), whichever is shallower, and upward integration of (17) is begun at that radius. This is sufficient to describe the depth-dependent deformation field for shallow sources, i.e. those within the uppermost elastic layer. If post-seismic deformation from deeper sources were sought, then the lower boundary condition would need to be applied at a deeper level and the free-surface boundary condition might need to be applied at some finite depth, depending on source depth. In the current version intended for application to shallow seismic sources, the procedure has been found to be stable with respect to a change in the starting depth of integration, as has been obtained previously in related investigations of static elastic deformation [Pollitz, 1996] and propagating waves [Friederich and Dalkolmo, 1995].

1.2 Toroidal Motion Solution

Specification of the solution for the toroidal mode component of deformation is analogous to that outlined here for the spheroidal mode displacement field. Working again in the Laplace transform domain, the total toroidal mode displacement field which solves (11) can be expanded as a sum of normal modes in the form

$$\mathbf{u}_T(\mathbf{r},s) = \sum_n \sum_{l=0}^{\infty} \sum_{m=1}^2 \frac{\left[-{}_n y_{1l}(r, s) \hat{\mathbf{r}} \times \nabla_1 \right]}{{}_n (I_1)_l ({}_n \omega_l)^2} \quad (30)$$

$$\times \Sigma_{m+3}(\phi, s) (-1)^m X_l^m(\theta) (1/s)$$

The corresponding traction on spherical shells of radius r can be written

$$\hat{\mathbf{r}} \cdot \mathbf{T}_T(\mathbf{r}, s) = \sum_n \sum_{l=0}^{\infty} \sum_{m=1}^2 \frac{\left[-{}_n y_{2l}(r, s) \hat{\mathbf{r}} \times \nabla_1 \right]}{{}_n (I_1)_l ({}_n \omega_l)^2} \quad (31)$$

$$\Sigma_{m+3}(\phi, s) (-1)^m X_l^m(\theta) (1/s)$$

As before, ${}_n (I_1)_l$ is the kinetic energy integral given by equation (11) of Pollitz [1992]. The source excitation functions are given by

$$\Sigma_4(\phi) = \left[\frac{l+1/2}{2\pi} \right] [l(l+1)]^{-1/2} (-M_{r\theta} \sin\phi + M_{r\phi} \cos\phi) [\partial_r y_1(r_s) - r_s^{-1} y_1(r_s)]$$

$$\Sigma_5(\phi) = \left[\frac{l+1/2}{2\pi} \right] [l(l+1)]^{-1/2} [(l-1)(l+2)]^{1/2} \quad (32)$$

$$\times \left[-\frac{1}{2}(M_{\theta\theta} - M_{\phi\phi}) \sin 2\phi + M_{\theta\phi} \cos 2\phi \right] r_s^{-1} y_1(r_s)$$

The displacement-stress vector

$${}_n \mathbf{y}_l = \begin{bmatrix} {}_n y_{1l} \\ {}_n y_{2l} \end{bmatrix} \quad (33)$$

obeys a matrix differential equation of the same form as (17), with \mathbf{y} and \mathbf{A} being 2×1 and 2×2 matrices, respectively. The differential equation which must be integrated from an appropriate starting radius up to the surface is

$$\frac{d\mathbf{y}_l(r)}{dr} = \mathbf{A}_{lv}(r) \mathbf{y}_l(r) \quad (34)$$

subject to boundary condition

$$y_2(R) = 0 \quad (35)$$

For spherical harmonic degree l and in layer v ,

$$\mathbf{A}_{lv}(r, s) = \begin{bmatrix} r^{-1} & \mu^{-1}(s) \\ r^{-2} \mu(s) (l-1)(l+2) & -3r^{-1} \end{bmatrix} \quad (36)$$

As in the case of spheroidal modes, each l component has a corresponding set of poles $s = -s_j$ for which $\omega^2(s)$ vanishes. In the toroidal mode case, displacement amplitudes are inversely proportional to

$$\varepsilon_j = I_1(s) \frac{d}{ds} \omega^2(s) \Big|_{s=-s_j} = \int_0^R I_1 \left[\frac{\partial \omega^2}{\partial \mu} \right] \Big|_{\kappa} \frac{\partial \mu(r, s)}{\partial s} dr \quad (37)$$

where

$$I_1 \left[\frac{\partial \omega^2}{\partial \mu} \right] \Big|_{\kappa} = \frac{1}{\mu^2} (r y_2)^2 + (l - 1) (l + 2) (y_1)^2 \quad (38)$$

The l component of the toroidal mode displacement field is then given by

$$\begin{aligned} \mathbf{u}_T(\mathbf{r}, t) = \sum_j [(\theta \gamma_T)_j(\mathbf{r}) \hat{\theta} + (\phi \gamma_T)_j(\mathbf{r}) \hat{\phi}] \\ \times \frac{1 - e^{-s_j t}}{s_j} \end{aligned} \quad (39)$$

where

$$\begin{aligned} (\phi \gamma_T)_j(\mathbf{r}) &= y_1(r, -s_j) \sum_{m=1}^2 \left[\Sigma_{m+3}(\phi, s) \partial_{\theta} X_l^m(\theta) (-1)^m \right] \epsilon_j^{-1} \\ (\theta \gamma_T)_j(\mathbf{r}) &= y_1(r, -s_j) \sum_{m=1}^2 \left[-\partial_{\phi} \Sigma_{m+3}(\phi, s) X_l^m(\theta) (-1)^m \right] \epsilon_j^{-1} (\sin \theta)^{-1} \end{aligned} \quad (40)$$

(2) Comments on Numerical Integration Method

Accurate calculation of postseismic relaxation fields depends on having an accurate method of integration of (17). The upward integration of (17) and application of surface boundary conditions may always be done stably in the toroidal mode case, but in the spheroidal mode case it is often an unstable process due to numerical dispersion which transforms linearly independent vectors \mathbf{y} at depth into nearly linearly dependent vectors at the surface. Integration schemes which ignore this effect can suffer from serious numerical problems. This problem must be considered in the computational method used to calculate relaxation here because it is based upon the identification of the characteristic decay times which form the basis of our normal mode approach. I have found that the integration of (17) can be done straightforwardly without numerical artifacts in the nongravitational case but that it leads to serious numerical dispersion and resultant misidentification of decay times in the gravitational case. In order to obtain stable results, the integration of (17) was done using the method of second-order minors.

In this method, originally developed by Gilbert and Backus [1966], two displacement-stress vectors $\mathbf{y}_1(r)$ and $\mathbf{y}_2(r)$ (assuming fixed l and with the s dependence implicit) are propagated upward from the starting radius of integration. The second-order minors $\{m_j\}$ are defined as follows [Takeuchi and Saito, 1972]

$$\begin{aligned}
 m_1(r) = m_{12} &= \begin{vmatrix} y_{11} & y_{21} \\ y_{12} & y_{22} \end{vmatrix}, & m_2(r) = m_{13} &= \begin{vmatrix} y_{11} & y_{21} \\ y_{13} & y_{23} \end{vmatrix} \\
 m_3(r) = m_{14} &= \begin{vmatrix} y_{11} & y_{21} \\ y_{14} & y_{24} \end{vmatrix}, & m_4(r) = m_{23} &= \begin{vmatrix} y_{12} & y_{22} \\ y_{13} & y_{23} \end{vmatrix} \\
 m_5(r) = m_{24} &= \begin{vmatrix} y_{12} & y_{22} \\ y_{14} & y_{24} \end{vmatrix}, & m_6(r) = m_{34} &= \begin{vmatrix} y_{13} & y_{23} \\ y_{14} & y_{24} \end{vmatrix},
 \end{aligned} \tag{41}$$

The minor m_6 is actually proportional to m_1 [Takeuchi and Saito, 1972]:

$$m_6 = -\frac{1}{l(l+1)} m_1$$

The differential equation (17) for these two displacement-stress vectors can be rewritten as a 5×5 system for the minors. Defining \mathbf{m} as the column vector with components m_j ($j = 1$ through 5), this equation takes the form (in layer v)

$$\frac{d\mathbf{m}(r)}{dr} = \overline{\mathbf{A}}_v \mathbf{m}(r) \tag{42}$$

subject to the surface boundary condition

$$m_5(R) = 0 \tag{43}$$

The elements of $\overline{\mathbf{A}}_v$ are linear combinations of the elements of \mathbf{A}_v and can be derived explicitly by combining (17) and (41) to rewrite (42) in the form

$$\frac{dm_{jk}(r)}{dr} = \sum_k (\mathbf{A}_v)_{jl} m_{lk} + (\mathbf{A}_v)_{kl} m_{jl} \tag{44}$$

Integration of (42) subject to the boundary condition (43) is necessary to obtain stable results in many applications in propagating wave seismology [Woodhouse, 1980; Friederich and Dalkolmo, 1995]. Its use here in the quasi-static deformation case is a natural extension of the methods given in those papers.

(3) Number of Mode Branches

Toroidal Modes

The free surface boundary condition (35) can be written in the form

$$\prod_{j=1}^M (s + s_j) = 0 \quad (45)$$

It can be proven [Pollitz, 1992] that all $s = -s_j$ must lie on the negative real axis, so M equals the number of characteristic decay times. Consider the set of layer boundaries dividing a viscoelastic spherical shell (i.e., one with finite η) from distinct purely elastic material above or below it. Let M_1 be the number of such boundaries, and let M_2 be the number of distinct homogeneous spherical shells with a Maxwell viscoelastic rheology (assuming for the moment that none of them possess a standard linear solid rheology). Then

$$M = M_1 + (M_2 - 1) \quad (46)$$

If the Earth model possesses at least one spherical shell with a standard linear solid rheology, then the number of zeros generally increases. Redefine M_2 to be the number of distinct homogeneous spherical shells with a viscoelastic rheology, inclusive of both a Maxwell viscoelastic and standard linear solid rheology. Let M_3 be the number of distinct homogeneous spherical shells with a standard linear solid rheology, and let M_4 be the number of layer boundaries dividing a spherical shell with Maxwell viscoelastic rheology from one with a standard linear solid rheology. Then

$$M = M_1 + (M_2 - 1) + (M_3 + M_4 - 1) \quad (47)$$

Spheroidal Modes

The free surface boundary condition (18) can also be written in the form (45). Define M_1 , M_2 , M_3 , and M_4 as above. If all viscoelastic layers have a Maxwell viscoelastic rheology, then

$$M = 3 M_1 + 4 (M_2 - 1) \quad (48)$$

If the Earth model possesses at least one spherical shell with a standard linear solid rheology, then

$$M = 3 M_1 + 4 (M_2 - 1) + 2 (M_3 + M_4 - 1) \quad (49)$$

It is interesting to note, in both the toroidal and spheroidal mode cases, that if the Earth model contains a single viscoelastic layer bounded above and below by purely elastic material, then the number of zeros M of (45) is independent of whether that layer possesses a Maxwell viscoelastic or a standard linear solid rheology -- if the layer is standard linear solid, then $M_3 = 1$ and $M_4 = 0$, so $M_3 + M_4 - 1 = 0$, and there is no difference in M between equations (46)/(47) or (48)/(49).

References

- Dahlen, F.A., Elastic dislocation theory for a self-gravitating configuration with an initial stress field, *Geophys. J. R. Astron. Soc.*, 28, 357-383, 1972.
- Cohen, S.C., A multilayer model of time dependent deformation following an earthquake on a strike slip fault, *J. Geophys. Res.*, 87, 5409-5421, 1982.
- Friederich, W., and J. Dalkolmo, Complete synthetic seismograms for a spherically symmetric earth by a numerical computation of Green's function in the frequency domain, *Geophys. J. Int.*, 122, 537-550, 1995.
- Gilbert, F., and G. Backus, Propagator matrices in elastic wave and vibration problems, *Geophysics*, 31, 326-332, 1966.
- Gilbert, F., and A.M. Dziewonski, An application of normal mode theory to the retrieval of structural parameters and source mechanisms from seismic spectra, *Philos. Trans. R. Soc. London, Ser. A*, 278, 187-269, 1975.
- Iwasaki, T., Quasi-static deformation due to a dislocation source in a Maxwellian viscoelastic earth model, *J. Phys. Earth*, 33, 21-43, 1985.
- Pollitz, F.F., Postseismic relaxation theory on the spherical Earth, *Bull. Seismol. Soc. Am.*, 82, 422-453, 1992.

- Pollitz, F.F., Coseismic deformation from earthquake faulting on a layered spherical Earth, *Geophys. J. Int.*, *125*, 1-14, 1996.
- Pollitz, F.F., Gravitational-viscoelastic postseismic relaxation on a layered spherical Earth, *J. Geophys. Res.*, *102*, 17921-17941, 1997.
- Pollitz, F.F. and I.S. Sacks, Viscosity structure beneath northeast Iceland, *J. Geophys. Res.*, *101*, 17771-17793, 1996.
- Romanowicz, B., Multiplet–multiplet coupling due to lateral heterogeneity: asymptotic effects on the amplitude and frequency of the Earth's normal modes, *Geophys. J. R. astr. Soc.*, *90*, 75-100, 1987.
- Rundle, J.B., Vertical displacements from a rectangular fault in a layered elastic-gravitational media, *J. Phys. Earth*, *29*, 173-186, 1981.
- Rundle, J.B., Viscoelastic-gravitational deformation by a rectangular thrust fault in a layered Earth, *J. Geophys. Res.*, *87*, 7787-7796, 1982.
- Takeuchi, H., and M. Saito, Seismic surface waves, in *Methods in Computational Physics: Seismology*, edited by B. Bolt, S. Fernbach, and M. Rotenberg, pp. 217-294, Academic Press, San Diego, Calif., 1972.
- Woodhouse, J.H., Efficient and stable methods for performing seismic calculations in stratified media, in *Physics of the Earth's Interior; Proceedings of the International School of Physics "Enrico Fermi", Course LXXVIII*, edited by A.M. Dziewonski and E. Bosci, pp. 127-151, North-Holland, New York, 1980.

(4) Validation

There are numerous factors which contribute to computed postseismic deformation for a given source: the discretization of the fault plane(s), the cutoff wavelength (equivalently, l_{\max}), the eigenfunction interpolation scheme, and the starting radius of integration of the radial eigenfunctions (equations (17) and (34)). In addition there is the implicit assumption that the propagator matrices \mathbf{P}_v used to construct the solution are correct.

The reliability of the theory and computations (non-gravitational case) are tested by comparison with independent semi-analytical and analytical results.

(1) **Relaxation following strike-slip faulting on an infinitely long fault.** The analytic solution to this problem on a homogeneous half-space is known (Savage and Prescott, 1978). To simulate this we construct a viscoelastic structure that has uniform elastic parameters (rigidity μ and Poisson's ratio 0.25) and an upper elastic shell underlain by an asthenosphere of viscosity η . We implement a very long vertical fault (length 1500 km) penetrating the entire elastic plate of thickness $H=30$ km. The maximum degree l_{\max} used in this (and subsequent) examples is chosen such that $2\pi R / l_{\max} = (2/3) \times H$ (R is Earth's radius). With y denoting the fault-parallel Cartesian coordinate and U the coseismic slip, we evaluate u_y / U at times $t=1\tau_0$ and $t=2\tau_0$, where $\tau_0 = \eta / \mu$ is the material relaxation time of the asthenosphere. Figure 2 demonstrates that the mode sum computed by VISCO1D matches the analytic solution very well.

(2) **Relaxation following dip-slip faulting on a finite fault.** We again construct a viscoelastic structure that has uniform elastic parameters (rigidity μ and Poisson's ratio 0.25) and an upper elastic shell of thickness H underlain by an asthenosphere of viscosity η . A finite fault that ruptures a very small portion of the elastic plate (at depth $0.786 \times H$) is prescribed length $20H/3$, rake 90° , and variable dip. We shall compare the mode sum with the "Direct Greens Function" (DGF) evaluation. In this

method, we implement the source directly using jumps in the displacement-stress vector at the source radius. In detail, we take the solution for static displacement on a spherically layered elastic model (Pollitz, 1996), change the shear modulus in the asthenosphere to a s -dependent modulus using the correspondence principle, and then evaluate the coseismic and postseismic displacements using a numerical inverse Laplace transform. Since the DGF method yields the coseismic displacement in addition to the postseismic displacement, we can also compare the DGF coseismic displacements with those computed analytically (e.g., Okada, 1992).

Let x and z be horizontal and vertical Cartesian coordinates (x measuring horizontal distance from the fault). Figures 3 through 5 show comparisons between the DFG solution and Okada solution for the coseismic displacement field along a profile that bisects the fault. Figures 6 through 8 show comparisons of post-thrusting relaxation between the mode sum and DGF solution. The comparison with the analytic coseismic displacements shows essentially that the DFG method implements the source correctly (and this point is made for several other cases in Pollitz, 1996) and that the program that carries out the DGF method is integrating along the fault plane correctly. These comparisons further suggest that the layer matrices used in the DGF method are correctly specified (both in theory and practice). In turn, since the static solution of the DGF method is constructed from the same layer matrices \mathbf{P}_v as those employed in the viscoelastic normal mode solution, we gain confidence in that part of the viscoelastic normal mode solution.

Figure 6 through 8 show very good agreement between the DGF solution and viscoelastic normal mode solution. I attribute slight differences to the numerical inverse Laplace transform used in the DGF method. The DGF method implements the source directly and does not identify the poles of the deformation functions in the Laplace transform domain. It computes Laplace-transformed deformation at a number of sample points in the complex s -plane and then estimates the excitation

of a number of decaying exponential functions corresponding to poles at specified collocation points on the negative real s -axis. The viscoelastic normal mode solution, on the other hand, identifies the poles of the Laplace-transformed deformation explicitly and evaluates their contributions analytically. The near-perfect agreement between the two very different methods demonstrates that VISCO1D is handling essentially all aspects of the post-thrusting case correctly.

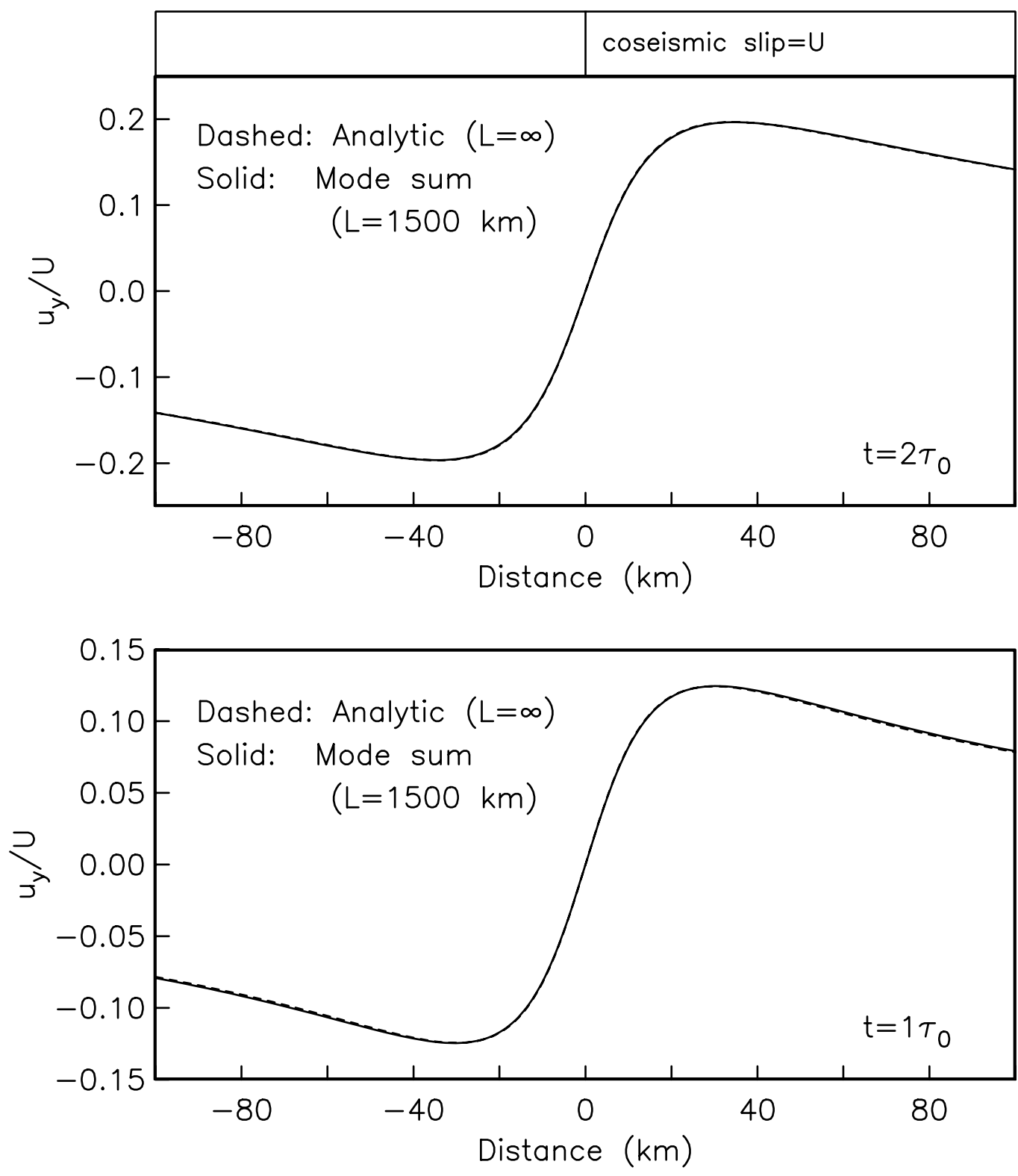
It is noteworthy that the post-thrusting case from a finite fault (case 2 above) has dominant contributions from the spheroidal model deformation field, whereas the post-strike-slip case for an infinitely long fault (case 1 above) has contributions exclusively from the toroidal mode deformation field. The comparison-results in these two cases jointly show that each of the separate toroidal and spheroidal components of the postseismic deformation field are being computed reliably.

References

- Okada, Y., Internal deformation due to shear and tensile faults in a half-space, *Bull. Seism. Soc. Am.*, 82, 1018-1040, 1992.
- Pollitz, F.F., Coseismic deformation from earthquake faulting on a layered spherical Earth, *Geophys. J. Int.*, 125, 1-14, 1996.
- Savage, J.C. and W.H. Prescott, Asthenospheric readjustment and the earthquake cycle, *J. Geophys. Res.*, 83, 3369-3376, 1978.

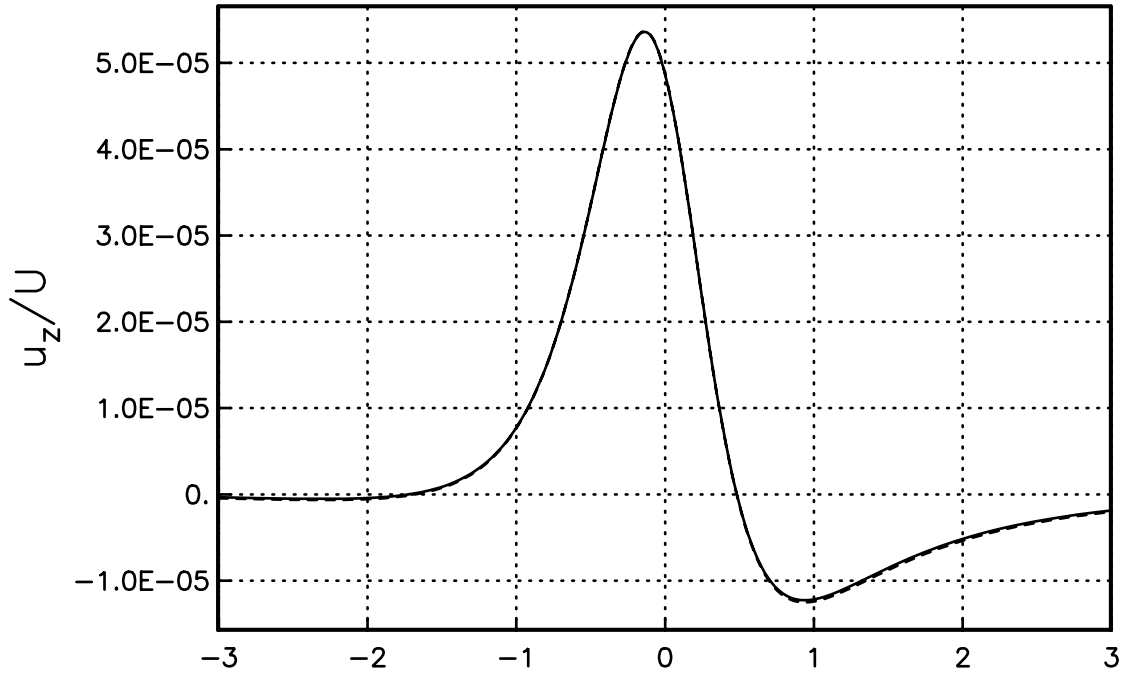
Figure 2

Postseismic fault-|| displacement



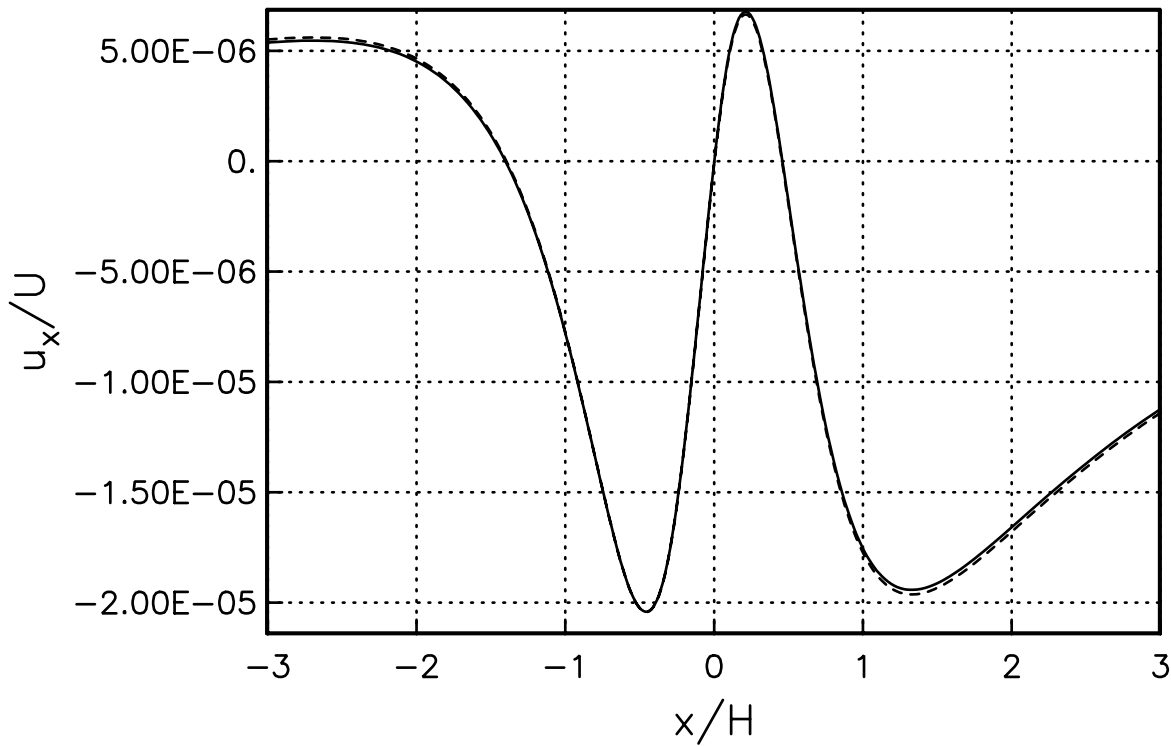
— Analytic (Okada)
- - - Direct Greens function

Vertical Displacement



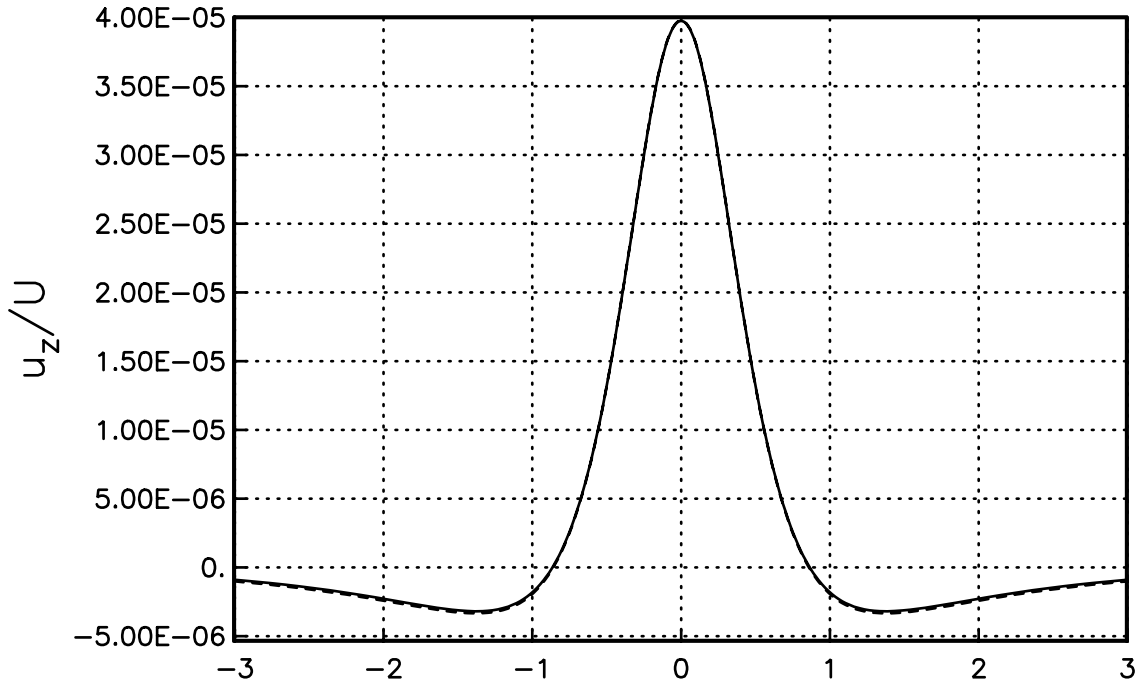
dip=30°
W=4.000e-3 x H
L=20H/3
Depth=0.786 x H
t=0+

Horizontal Displacement



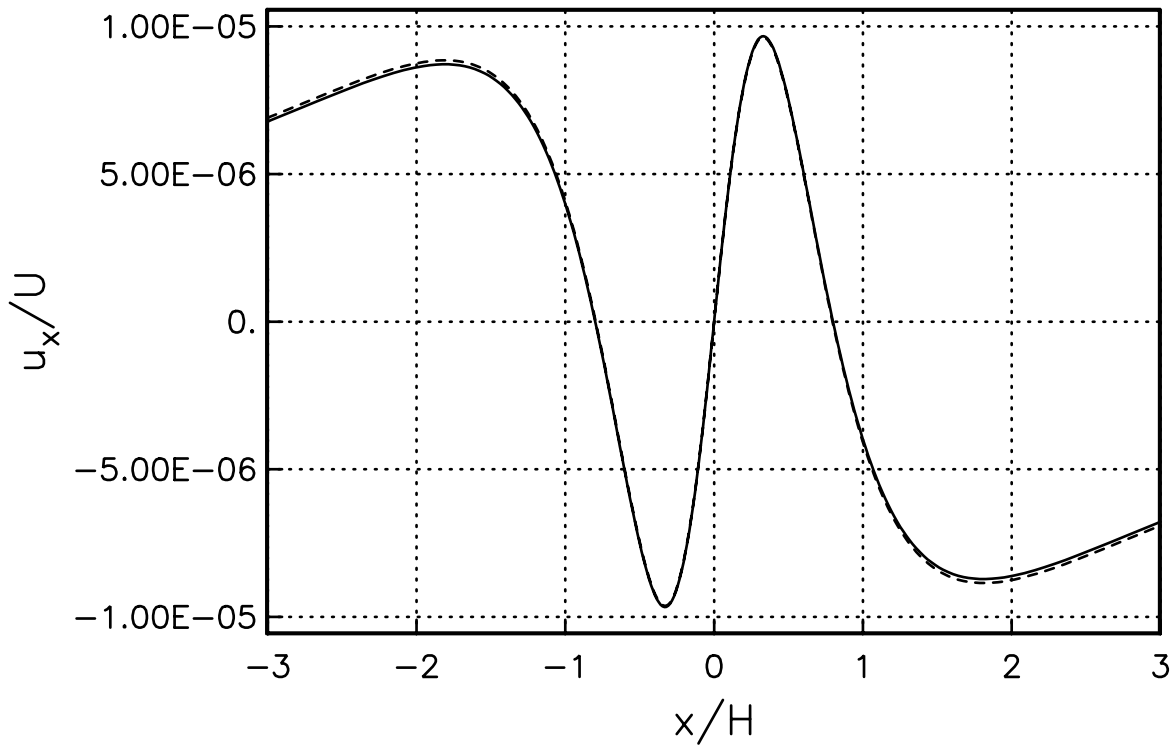
— Analytic (Okada)
- - - Direct Greens function

Vertical Displacement



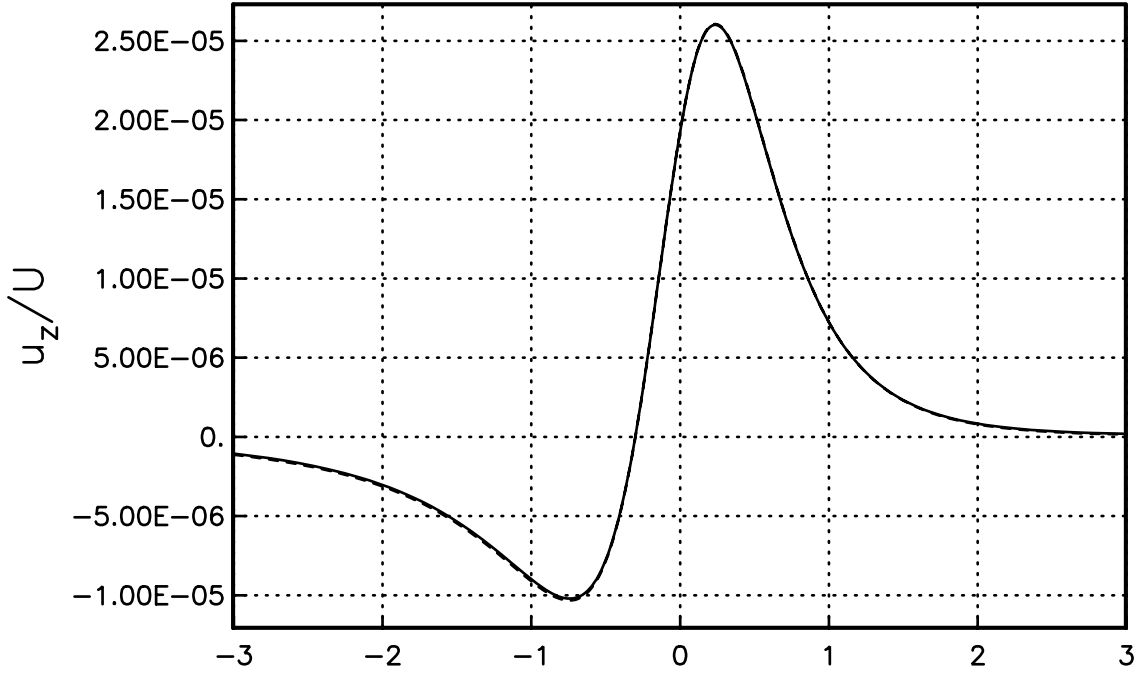
dip=45°
W=2.828e-3 x H
L=20H/3
Depth=0.786 x H
t=0+

Horizontal Displacement



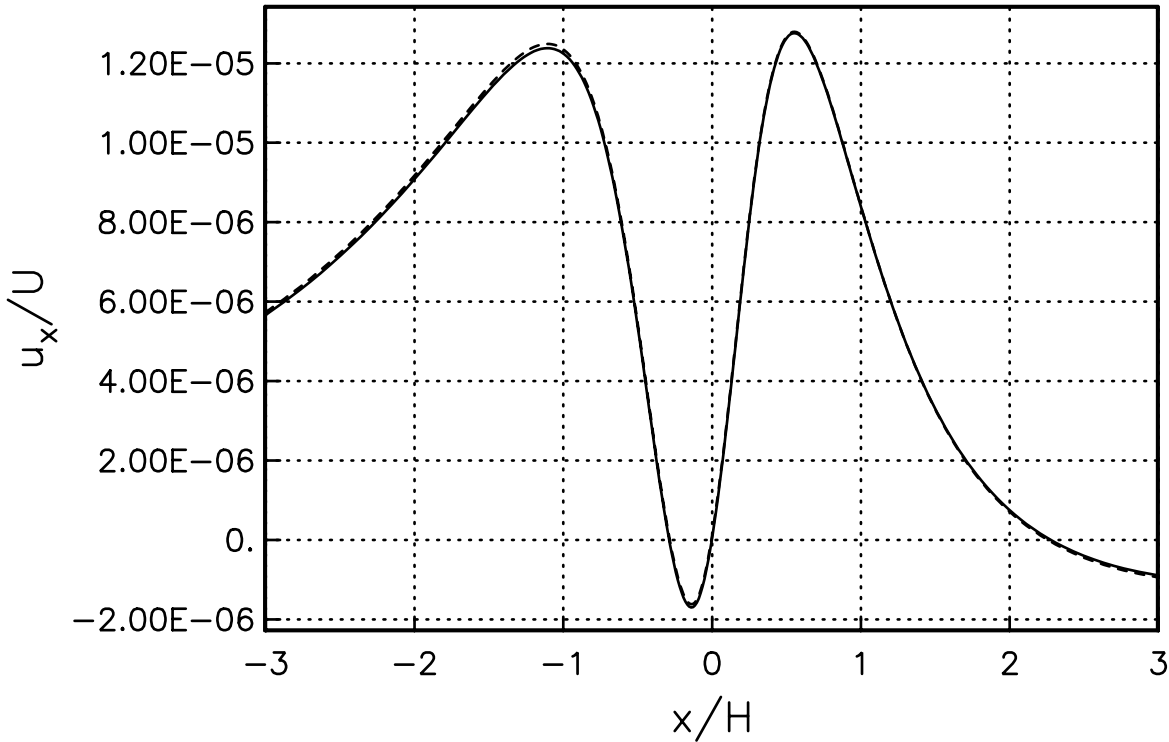
— Analytic (Okada)
- - - Direct Greens function

Vertical Displacement



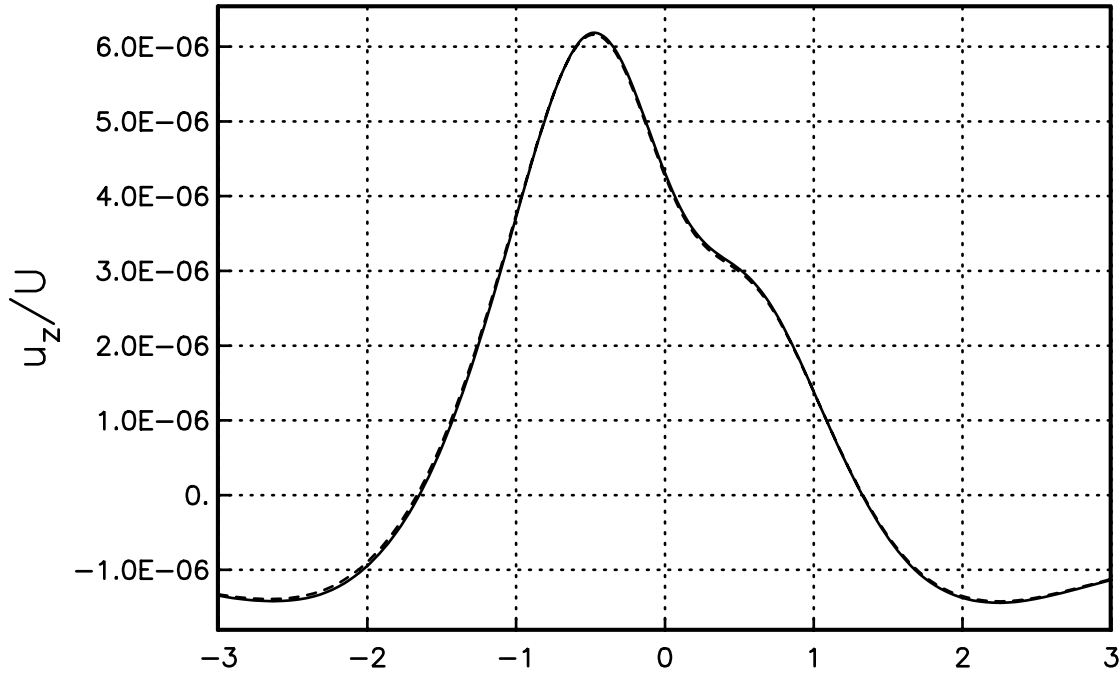
dip=70°
W=2.128e-3 x H
L=20H/3
Depth=0.786 x H
t=1 τ_0

Horizontal Displacement



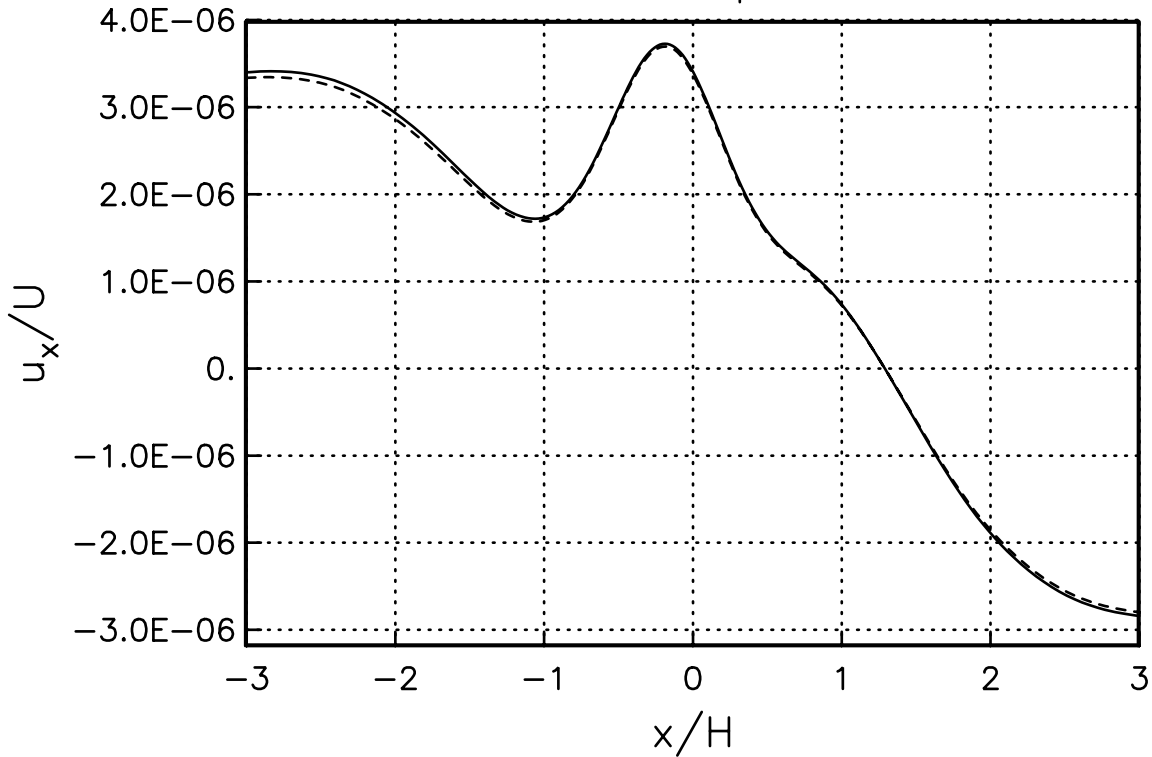
— Mode sum
- - - Direct Greens function

Vertical Displacement



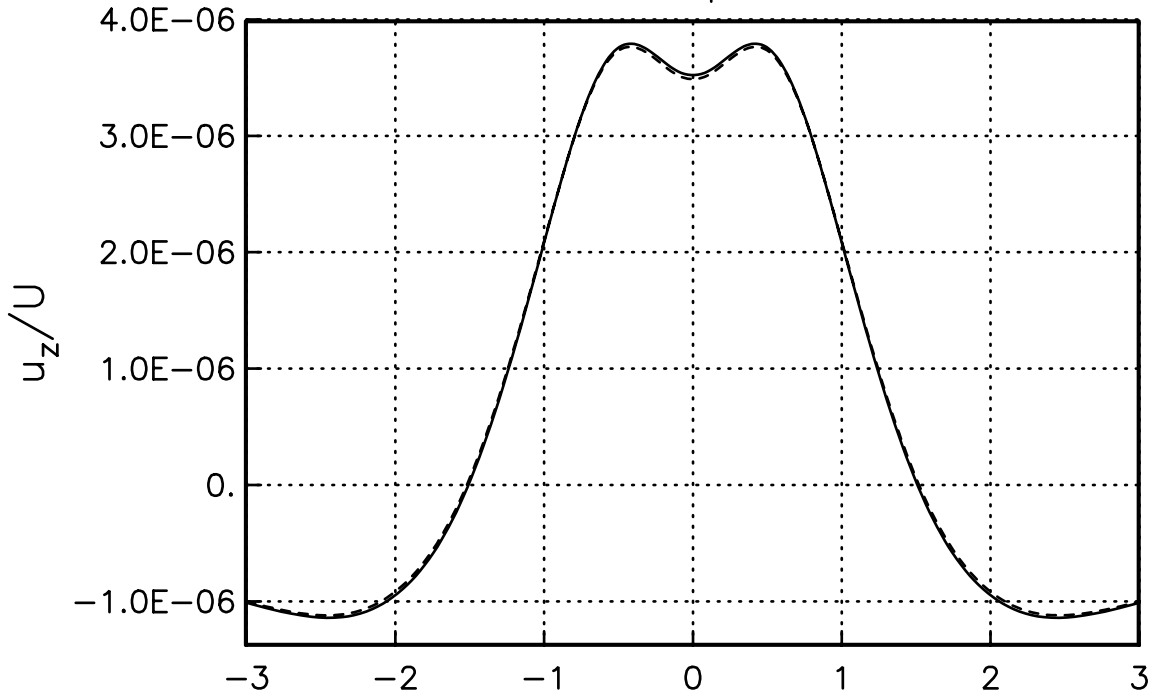
dip=30°
W=4.000e-3 x H
L=20H/3
Depth=0.786 x H
t=1 τ_0

Horizontal Displacement



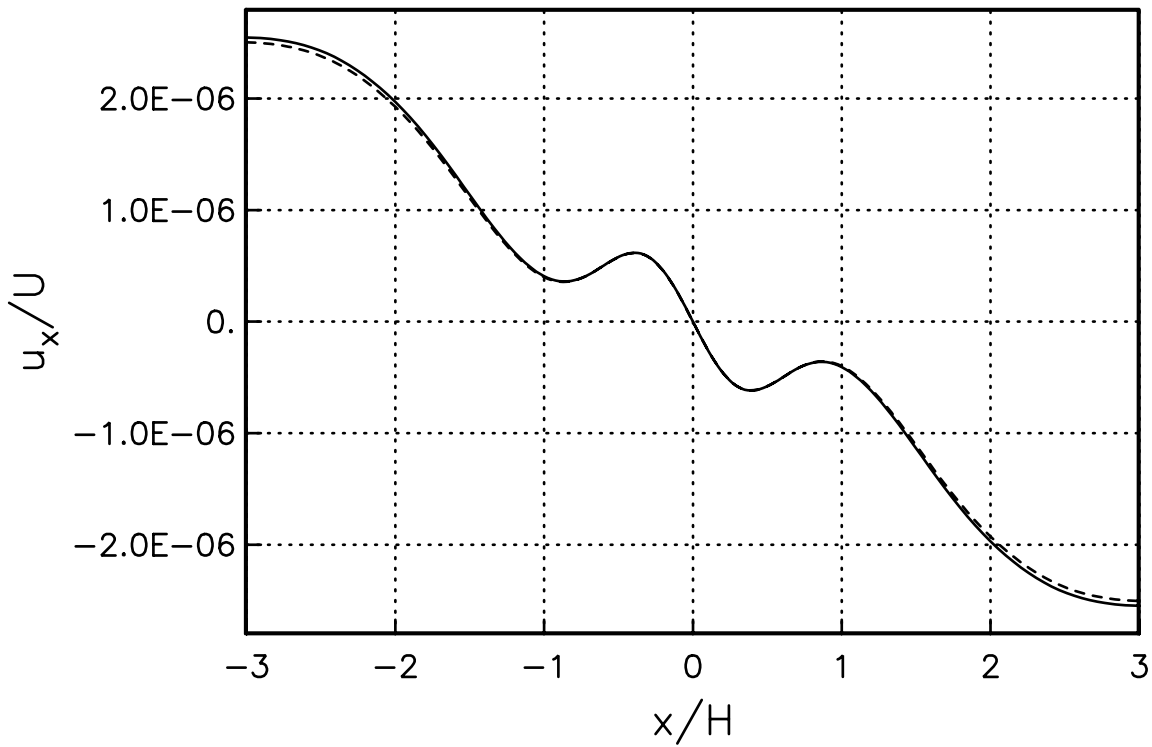
— Mode sum
- - - Direct Greens function

Vertical Displacement



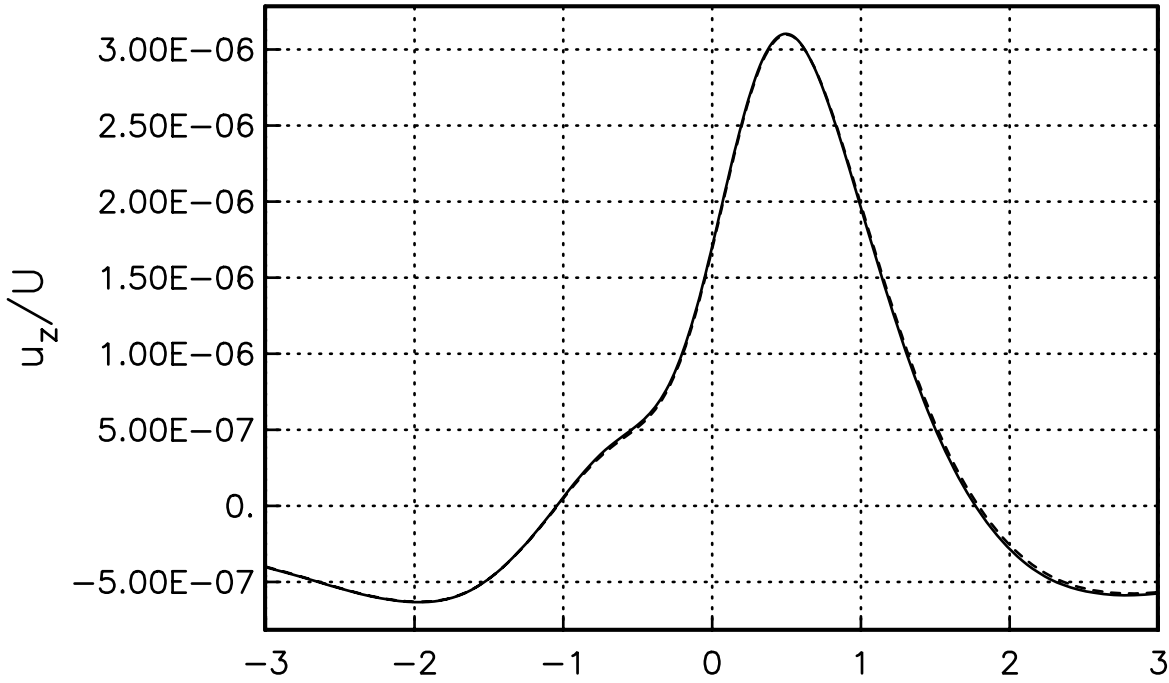
dip=45°
W=2.828e-3 x H
L=20H/3
Depth=0.786 x H
t=1 τ_0

Horizontal Displacement



— Mode sum
- - - Direct Greens function

Vertical Displacement



dip=70°

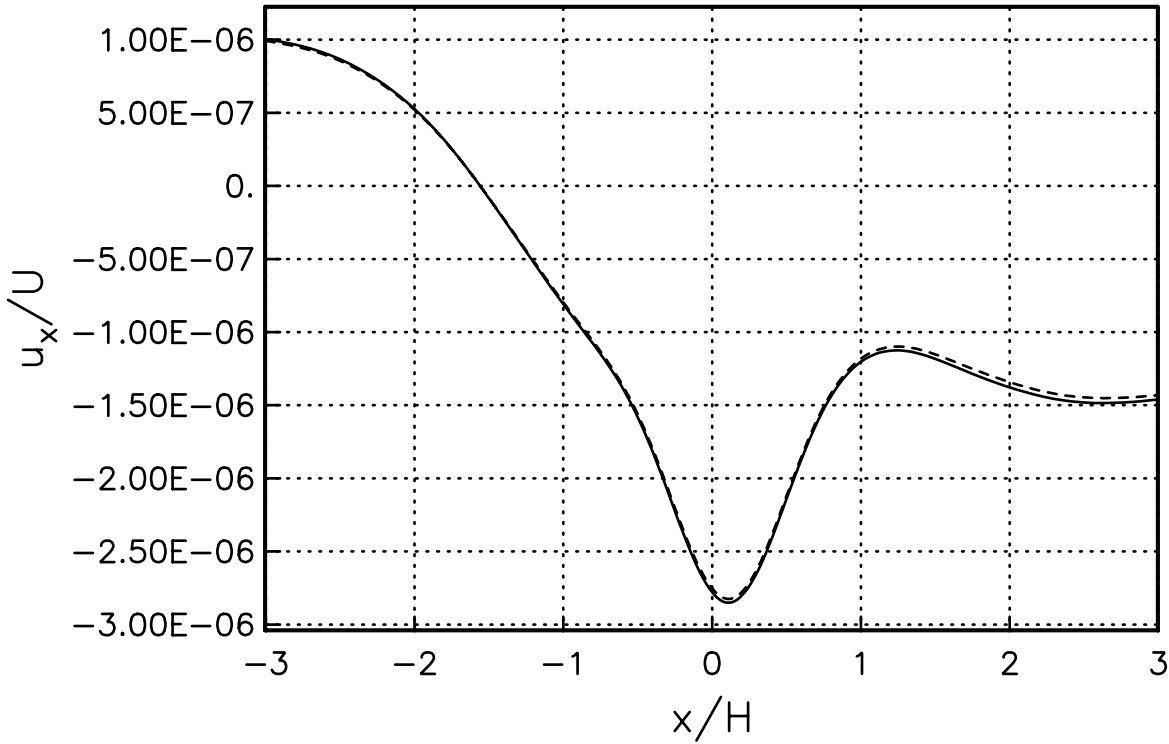
$W=2.128e-3 \times H$

$L=20H/3$

Depth=0.786 x H

$t=1\tau_0$

Horizontal Displacement



(5) Organization of the Programs

All source code for the viscoelastic relaxation programs and several examples for calculating postseismic deformation are in the /viscoprogs directory.

The programs are organized as follows:

Purpose	TOROIDAL MOTION program	SPHEROIDAL MOTION program
Determine characteristic decay times	decay	decay4 or {decay4m,decay4g}
Determine corresponding eigenfunctions	vtordep	vsphdep or {vsphg}
Determine time-dependent postseismic velocity or cumulative postseismic displacement for specified fault plane(s) & observation points	strainx	strainw

Comments:

1. DECAFY and DECAFY4 have a common standard input file which specifies the **minimum and maximum spherical harmonic degree used in the deformation field expansion**. They both read in **viscoelastic stratification** and other information about the Earth model from an input file called 'earth.model', as described in the examples in the *Tutorial*. For each spherical harmonic degree, the programs find zeros $s = -s_j$ of a function (equation (18) for spheroidal modes; equation (35) for toroidal modes) by dividing the negative s -axis into numerous short segments and systematically searching for zero crossings of this function.
2. VTORDEP and VSPHDEP read in files created previously by DECAFY and DECAFY4, respectively, as well as the **depth at which deformation results are to**

be calculated from standard input. VTORDEP obtains and writes out the eigenfunctions $y_1(r, -s_j)$ and $\partial_r y_1(r, -s_j)$ (section 1.2), and VSPHDEP obtains and writes out the eigenfunctions $y_1(r, -s_j)$, $\partial_r y_1(r, -s_j)$, $y_3(r, -s_j)$, $\partial_r y_3(r, -s_j)$ (section 1.1), over the depth range originally specified in 'earth.model'.

3. STRAINX and STRAINW read in files created previously by {DECAY,VTORDEP} and {DECAY4,VSPHDEP}, respectively, and they read from standard input the **number of fault planes, geometry and slip of each fault plane, location of observation points, time of earthquake, whether postseismic velocity at one time or cumulative postsesimic displacement between two times is desired, and start/end time of deformation to be evaluated (needed if cumulative displacement is desired)**. Either **surface deformation** or **deformation at a specified depth** can be calculated.

4. STRAINX and STRAINW divide each fault plane into (nmesh1-1) X (nmesh2-1) nonoverlapping rectangles, with **nmesh1** and **nmesh2** specified in the source code 'strainx.f' and 'strainw.f'. When the fault dips 90 deg. then it saves a lot of time to set nmesh1=2 in these programs, but when a fault does not dip 90 deg. then nmesh1 should be large enough that the fault is well divided in the along-dip direction. Similarly, nmesh2 should always be chosen so that the fault is well divided in the along-length direction. I end up changing these values for almost every application, and I typically choose nmesh1 and nmesh2 so that the separation between adjacent rectangles is a fraction of the elastic plate thickness; what values to choose is worth considering because computation time is proportional to (nmesh1-1) X (nmesh2-1). The maximum value of nmesh1 which should be used is 41.

5. The final output of STRAINX and STRAINW has all three components of displacement (or velocity) and all six components of the strain (or strain rate) tensor at all of the specified observation points.

6. The programs described above handle the non-gravitational case. Programs DECA4M, DECA4G, and VSPHG are needed for the gravitational case. Most examples given in the *Tutorial* use only the nongravitational programs because they generally run much faster than the gravitational programs.

7. One of the input parameters in the algorithm is **Earth's radius**. It is allowed to be variable in the non-gravitational programs. In the spherical harmonic summation method which is employed, using a radius smaller than Earth's true radius (6371 km) can speed things up considerably because, for a given cutoff wavelength, a smaller maximum spherical harmonic degree can then be used. There are two issues involved with using any radius < 6371 km. First, one should be sure that sphericity effects are not important for the problem at hand (this can be addressed by experimenting with different radius values). One of the consequences of using a smaller radius is that programs STRAINX and STRAINW will then assume that a point A (i.e. source) - point B (i.e. observation point) azimuth evaluated locally at point A exactly equals the negative of the point B - point A azimuth evaluated locally at point B. The former is needed to describe the directivity of the various source excitation functions at point A, while the latter is needed to rotate spherical strain components into local Cartesian strain components at point B. If sphericity effects are significant enough that the above equality does not approximately hold, then use radius = 6371 km. Second, the gravitational programs DECA4M, DECA4G, and VSPHG must be run with radius = 6371 km.

(6) Troubleshooting

This program package has yielded extremely stable results in all simulations which I have attempted over the past several years. Nevertheless, when I occasionally overstep the bounds intended for the programs, I will encounter wildly inexplicable results (i.e., overflow, segmentation errors) before I discover the mistake. Below I give a few examples that should cover most of the potential problems.

1. Overflow is encountered when running DECAFY or DECAFY4 or DECAFY4M, and the overflow yields NaN in output files. The most common reason for this is that one or more layer thicknesses in 'earth.model' is too large. Both DECAFY and DECAFY4 work with analytical layer matrix solutions for elastic deformation within each layer, and these solutions behave as $\sim (r/r_0)^{\pm l}$, where r_0 is a reference radius for that layer. If the ratio of the top to bottom radius of the layer is too large, and the spherical harmonic degree number l is sufficiently large, then overflow will result. The solution is to subdivide the (largest) layers in 'earth.model' into smaller layers.

2. Extremely large deformation values or segmentation errors are encountered when running STRAINX or STRAINW. This most likely results when more than 4 distinct viscoelastic layers are specified in 'earth.model' (several consecutive layers with identical elastic and viscoelastic parameters count as 1 "distinct" layer). This generates potentially more than 4 distinct relaxation times per spherical harmonic degree for toroidal modes, and more than 15 distinct relaxation times per spherical harmonic degree for spheroidal modes. If this is the problem, then either (1) limit the number of distinct viscoelastic layers to 4 or fewer, or (2) manually change the value of the parameter maxmod to a greater value in vtordep.f, strainx.f, vsphdep.f, and strainw.f

3. Other problems may be encountered if the following limits are exceeded:

- (1) Do not use more than 100 total layers in 'earth.model'
- (2) Do not evaluate deformation for more than 1600 points at a time (i.e., number of observation points in input file to STRAINX, STRAINW).
- (3) Do not evaluate deformation for more than 150 fault segments at a time (i.e., number of fault segments in input file to STRAINX, STRAINW).
- (4) Do not use a value of nmesh1 greater than 41 in strainx.f or strainw.f
- (5) Do not use a spherical harmonic degree less than 2 or greater than 2500 (i.e. l_{\min} and l_{\max} in input file to DECAY or DECAY4 or DECAY4M).
- (6) Always use Earth radius=6371 km in 'earth.model' when the gravitational programs DECAY4M, DECAY4G, and VSPHG are used.

4. Too few mode branches seem to be found by DECAY or DECAY4 (or DECAY4M). This occurs for a good reason at larger spherical harmonic degrees l . Because the intended applications involve shallow earthquake sources, the equations of static equilibrium are integrated upward starting from a nominal starting radius -- about 2 wavelengths deep (if Earth's radius is 6371 km and $l = 1000$, then one wavelength is 40 km, so numerical intergration is begun 80 km down, with a lower boundary condition corresponding to homogeneous material below that depth). This means that any modes found will be insensitive to depth-varying elastic or viscoelastic structure deeper than 80 km. It is clear from the mode counting formulas (section 3) that, if there is depth-varying structure below 80 km depth, then a number of mode branches will "fall out" at this particular l as a result. Because the seismic source is shallow, however, the missed modes correspond to local deformation near a deep boundary, with very small eigenfunctions at the source depth, so that the source excitation functions Σ_m (equations 16 and 32 of section 1) are extremely small. Another reason that mode branches may be missed is that the search for zeros of the surface boundary condition (equation 45 of section 3) may use steps in the s -domain which

are too large, causing the program(s) to skip over 2 closely-spaced mode branches altogether. If you suspect that this is the case, then manually change the value of "nfrac(1)" in decay.f, decay4.f, and/or decay4m.f to a larger value (the computation time will correspondingly increase).